Recent advances in Sensors applications using AZO and GZO as Plasmonic material in IR and NIR frequency region

Sukla Rajak^{1*}

¹M.U.C. Women's College, Bardhaman, West Bengal 713104, India

E-mail:sukla.phy@gmail.com

(Received: July 11, 2024, Revised: August 21, 2024, Accepted: August 26, 2024, Published: September 30, 2024)

Abstract: Transparent conducting oxides become the promising alternative material to the conventional metals in the application of plasmonic materials in recent advances in Sensors in NIR and telecommunication frequency region. The optical and electric properties of TCOs have been explored for the study of plasmonic and MM devices as substitute to metals. Heavily doped Zinc oxides have the optical and electrical properties suitable for this application in the optoelectronic Sensors in the optical range based on surface Plasmon resonance. Aluminium doped Zinc oxide and Gallium doped Zinc oxide have the promising application in the field of Surface Plasmon resonance is mostly depending on the thickness of the TCO material and the angle of incidence of the incident exciting electromagnetic light. This study aims to report the study of Aluminium doped ZnO (AZO) and Gallium doped ZnO (GZO) for the propagation of surface Plasmon polariton wave with several thickness and angle of incidence, supported by MATLAB simulations and their application in the recent advances in optoelectronic Sensors.

Keywords: AZO, GZO, optoelectronic Sensors, Surface Plasmon Resonance

I Introduction

New Plasmonic materials provide several advantages in the field of optoelectronic devices and solar cells (1),(2),(3). Those plasmonic materials provide low intrinsic loss, ease in semiconductor-based design. They are compatible with standard nanofabrication processes. Transparent conducting oxides such as Al: ZnO, Ga:ZnO and indium-tin-oxide (ITO) enable many high-performance meta-material devices operating in the near-IR region. In recent plasmonic applications in NIR-IR region, Al doped Zinc oxides and Ga doped zinc oxides (ZnO:Ga) become alternatives to conventional metals and indium tin oxide (ITO). Transparent conducting oxides [Brewer, 2004] thin films are greatly used in plasmonic devices as they have good conductivity, appreciably high optical transmittance over the visible wavelength region, excellent adhesion to substrates, chemical stability, and photochemical properties. Among all the metal oxides, several studies have been reported on the use of ITO (4; 5; 6; 7; 8; 9; 10). Along with ITO, ZnO: Al and ZnO:Ga are important substitute to metals in recent developments of optoelectronic devices. AZO and GZO thin films possess some extraordinary advantages such as lower cost, thermal stability and comparatively low deposition temperature with greater stability under hydrogen plasma bombardment. It can exhibit tunable optical properties.

Zinc Oxide can be used as low loss plasmonic materials(11; 12; 13; 14; 15). Having wide band gap and negative permittivity in the frequency range and under certain circumstances. In the telecommunication wavelength AZO and GZO have lower loss. The electrical and optical properties of ZnO are changed dramatically with the introduction of group III elements such as Al, Sn, Ga into intrinsic ZnO. In this paper the variation of Resonance spectra with the variation of thickness of the metal oxide thin film (AZO and GZO) and the angle of incidence at which the exciting beam incident on the Kretschmann Configuration is presented and the application of AZO and GZO in biosensors are described in details considering the FWHM of the Reflectance Spectra.

DOI: 10.5281/zenodo.15710918 Page 1

II Conventional SPR Structure (Kretschmann configuration) for excitation of Surface Plasmons:

The coupling between the conduction electrons of the materials with the interacting electromagnetic waves is described by the classical Drude theory according to which the complex electrical permittivity is described by

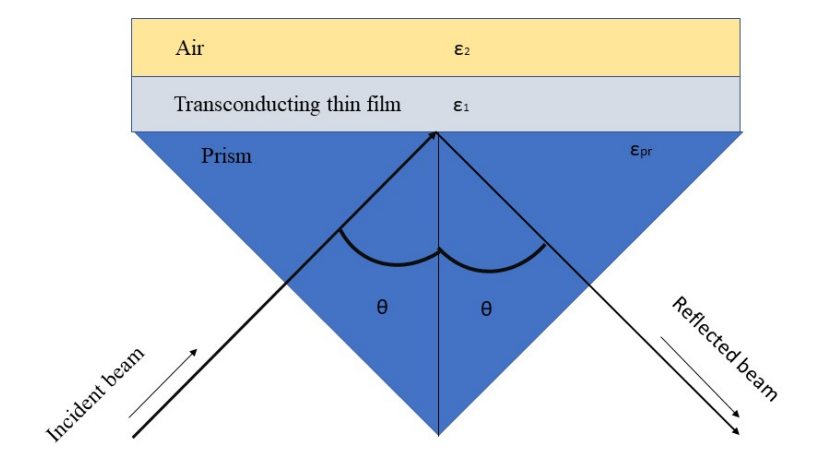
$$\varepsilon = \varepsilon' + i\varepsilon'' = \varepsilon_{\infty} - \frac{\omega_p^2}{\omega(\omega + i\gamma)}$$
(1)

Where, ε_{∞} is the high-frequency dielectric constant, γ is the damping coefficient of free electrons, and ω_p is the plasma frequency. For low loss, the material should have a small γ value.

Plasma frequency is defined as:

$$\omega_p = \sqrt{\frac{ne^2}{\varepsilon_0 m^*}} \tag{2}$$

where n is the free electron density, e is the elementary charge, ε_0 is the permittivity of free space, and m^* is the effective mass of the electron.



Kretschmann Configuration (substrate/overlayer/ambient)

Figure 1: Kretschmann configuration in three-layer model.

Figure 1 demonstrate the Kretschmann configuration, where the p-polarised electromagnetic radiation propagating through the prism is incident on the metal prism interface and an evanescent wave is generated at the interface. When the ATR condition is achieved then light is totally reflected internally and in the perpendicular direction to the interface of the prism and the metal oxide layer, the evanescent waves decay exponentially. In this three-phase model, the dielectric constant of prism is ε_p and the dielectric constant of the surrounding medium is ε_2 and θ is the angle of incidence and the resonant

light tunnels through the metal oxide film and results in coupling of light with the Surface Polaritons. At this resonant condition, there is a sharp dip in the reflectance at the detector.

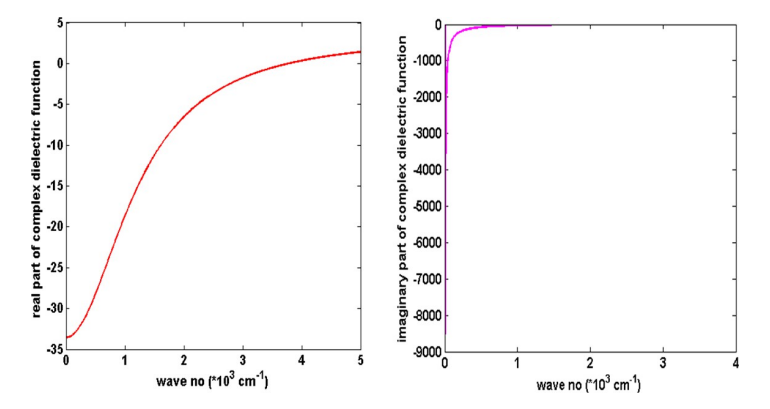


Figure 2: Variation of real part and imaginary part of complex dielectric function with the wave number of the incident exciting radiation for ZnO: Al layer.

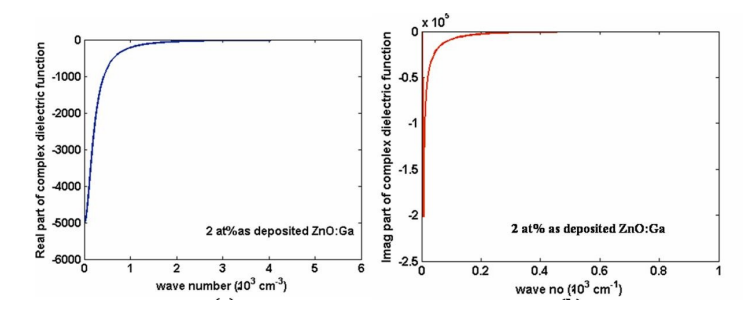


Figure 3: Variation of real part and imaginary part of complex dielectric function with the wave number of the incident exciting radiation for 2 at as-deposited ZnO:Ga.

In this configuration, the prism with dielectric constant ε_p is illuminated by the incident light. The dielectric constant of the prism will be greater than the dielectric constant of the surrounding medium, ε_2 ($\varepsilon_p > \varepsilon_2$). At a small angle of incidence, a portion of light is reflected at a bottom of the prism and some portion of light is refracted at the interface of prism and metal oxide layer. This optical phenomenon of Reflection and refraction are analyzed assuming the plane wave incident light. For TIR (total internal reflection), the critical angle will be,

$$\theta_c = \sin^{-1} \sqrt{\frac{\varepsilon_2}{\varepsilon_p}} \tag{3}$$

At the angle of incidence θ at which the resonant light tunnels through the metal oxide film and results in coupling of light with the Surface Polaritons. At this resonant condition, there at the detector there is a sharp dip in the reflectance. The intensity of the reflected light reaches its minimum value at a particular angle or wavelength, and it is demonstrated by a sharp dip in the SPR curve. Surface Plasmon Resonance is dependent on energy of incident radiation, thickness of metal or metal oxide film and angle of incidence and described by the three phase Kretschmann (substrate/ overlayer/ ambient) model (16). This Kretschmann representation is sensitive for thin film, for larger thicknesses this structure gradually weakens, in agreement with theory. No other collective excitations are observed. At the interface of Al doped Zinc oxide and Ga doped Zinc oxide film and BK7 glass, the Surface Plasmon

Polaritons are excited in the near infra-red wavelength $(1.45 \ddagger m - 1.59 \ddagger m)$ region (17) important optical wavelengths for plasmonic applications (1),(2).

In this study three phase layer Kretschmann Configuration is used to detect Surface plasmons in metal oxide thin film. If the field reflectance at metal oxide layer- prism interface is rp1 and the field reflectance at air- metal oxide interface is r12 then this field reflectance can be determined from the following equations

$$r_{p1} = \frac{\cos \theta / n_p - \left(\sqrt{\varepsilon_1 - n_p^2 \sin^2 \theta}\right)}{\cos \theta / n_p + \left(\sqrt{\varepsilon_1 - n_p^2 \sin^2 \theta}\right)}$$
(4)

$$r_{12} = \frac{\left(\sqrt{\varepsilon_2 - n_p^2 \sin^2 \theta}\right) / \varepsilon_2 - \left(\sqrt{\varepsilon_2 - n_p^2 \sin^2 \theta}\right) / \varepsilon_2}{\left(\sqrt{\varepsilon_2 - n_p^2 \sin^2 \theta}\right) / \varepsilon_2 + \left(\sqrt{\varepsilon_2 - n_p^2 \sin^2 \theta}\right) / \varepsilon_2}$$
 (5)

III Results and Discussions

III.a SPR Reflectance Profile for AZO

The SPP resonance curves are shown in Figure 3 for ZnO: Al as a function of frequency and for incident angle from 42° to 69° with 30 increments in the 1.55-micron wavelength window. The figure consists of nine subsections with variation of thickness of trans-conducting film under consideration.

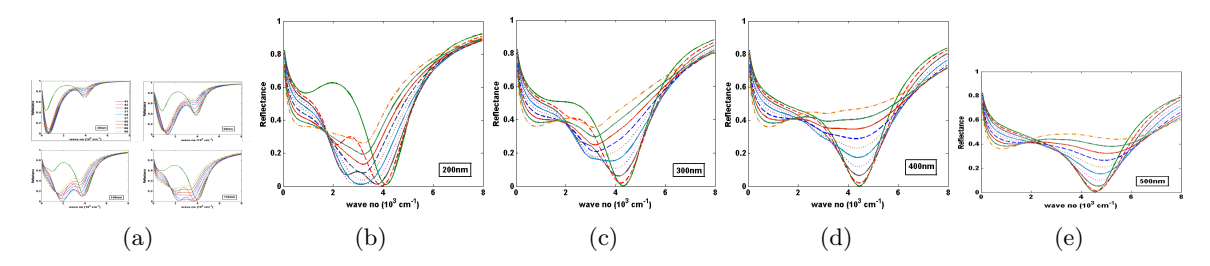


Figure 4: Reflectance vs wave number curves for different thicknesses of ZnO: Al film from 20 nm to 500 nm, with *theta* varying from 42° to 69° in steps of 30

Here, from the theoretical data we have found that the angle of incidence at which resonance occurs is 420 for ZnO: Al. With every increment of theta the SBPP resonant frequency does not alter though the reflectivity increases to some extent. With increased thickness, for 100 nmZnO: Al, at resonant frequency, reflectivity dip (in between 2000 cm - 1 to 4000 cm - 1) almost approaches zero, signifies that plasmons are efficiently coupled to incident light. With further increase of the film thickness, the SBPP resonance appears to behave differently. The resonant frequency shifts to higher energies for lower incident angle (3820 cm-1 for 420) and to lower energies for higher incident angle (1698 cm-1 for 480) and beyond that resonant energy is found to be almost independent of theta, which corresponds to SPP resonance. From the reflectance vs wave no curves for different thickness panels, it can be observed that SPP coupling is optimum for 150 nm thickness. If the thickness of the Al doped Zinc oxide coating is 500nm thick, then it is noticed that only lower angles can support SPP excitation although not much efficient, and for theta above 480, practically there is no coupling between plasmons and incident radiation. In Figure 3, dual resonance dips are noticed with varying reflectance minima values for thickness below 100 nm. Here this type of resonance is called Fano resonance or asymmetric

type of dual dips. In this simulation, it is noticed that for theta > 510, the reflectance profile does not correspond to SPP excitation of interest. For 30~nm ZnO: Al film, dual dips having minima at 954~cm-1 and 3873~cm-1 corresponding to angle 510~and~430 respectively. The reflectance profile is deeper for lower incident angle for second dip. Again, for 500~nm thickness, resonance curve become symmetric type with one reflecting dip. From these reflectance profiles it is showed that the optimized angle of incidence for 100nm Al doped ZnO is 480~and for 200nm AZO it is 430. At this angle of incidence, the exciting radiation coupled with the Surface Plasmons and the reflectance detected at the detector is minimum.

III.b Analysis for conventional SPR structure in 2.5 μm range:

The variable nature of Reflectance with the angle of incidence of the exciting radiation for Al doped ZnO support the SPP excitation in the mid infra-red (2.5 micron) wavelength range depicted in Figure 4. Figure 4 is the two-dimensional variation of Reflectivity with frequency for different thicknesses from 30nm (pink line) to 500nm (violet line) when exciting radiation incident at an angle 450 to the metal oxide layer. Minimum reflectivity position for ZnO: Al is lower or in other words, corresponds to higher absorbance of incident light. Above 200nm thickness, ZnO: Al gives almost 100% absorption.

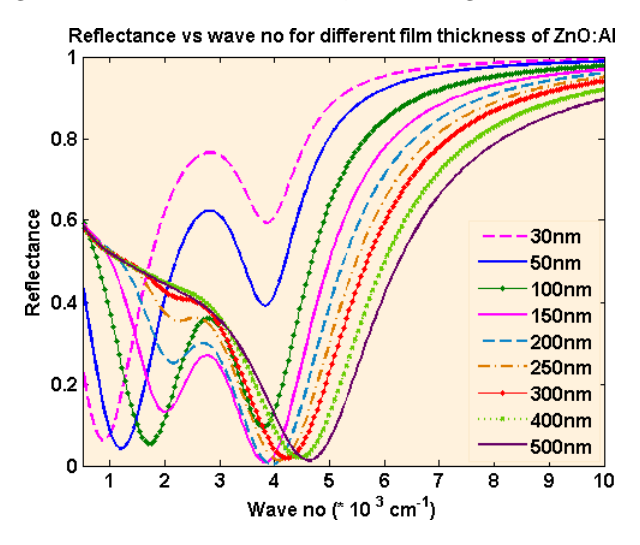


Figure 5: Variation of Reflectance profile with different increasing thickness of ZnO: Al (from 30 nm to 500 nm) at 45° incident angle.

III.c Sensor performance of AZO and related sensitivity issues:

Figure 9 shows the sensitivity responses of Al doped Zinc oxides in IR and NIR optical regions. These are the reflectance curves with the incident light wave number for different samples whose refractive indices are mentioned in the legend of the curves shown in (a) and (b). The shift in the wave number due to change in the refractive index of the sample is very small. In this study, the sensitivity is calculated as the change in the wave number at resonance due to change of the refractive index of the sample. We have theoretically studied sensing of different gaseous samples using the proposed structure taking air as reference. We investigated the sensitivity of 150 nm thick ZnO: Al in the 1.55-micron frequency range and 250 nm thick ZnO: Al film in 2.5-micron frequency range. The dip shift on the reflection spectrum is used to detect the sample in terms of refractive index. Zoomed insets of the corresponding dips are used to calculate sensitivity. The resonance wave number shifts to higher value when sample refractive index increases. This implies that measurements with ZnO: Al thin film layer is sensitive in both and can be used as sensing materials in case of sensors. One of the prospective approaches to further improving the sensing technique involves both detection accuracy and sensitivity.

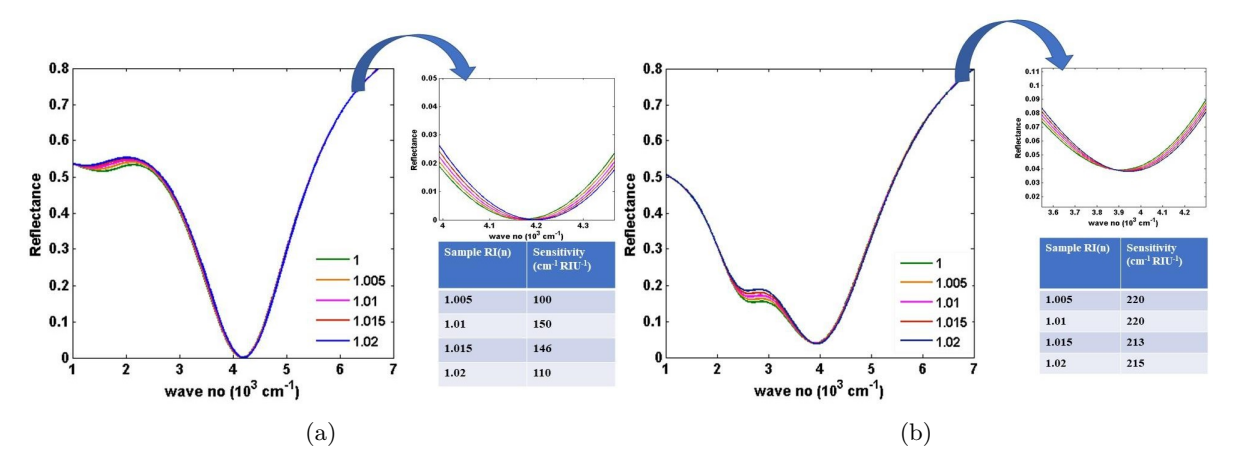


Figure 6: Sensing of gaseous samples using ZnO: Al film in (a) 1.55 micron (b) 2.5-micron incident frequency range

The sensitivity response of Al doped Zinc oxides for the different ambient material like gaseous and liquid based are also studied in Figure 11.

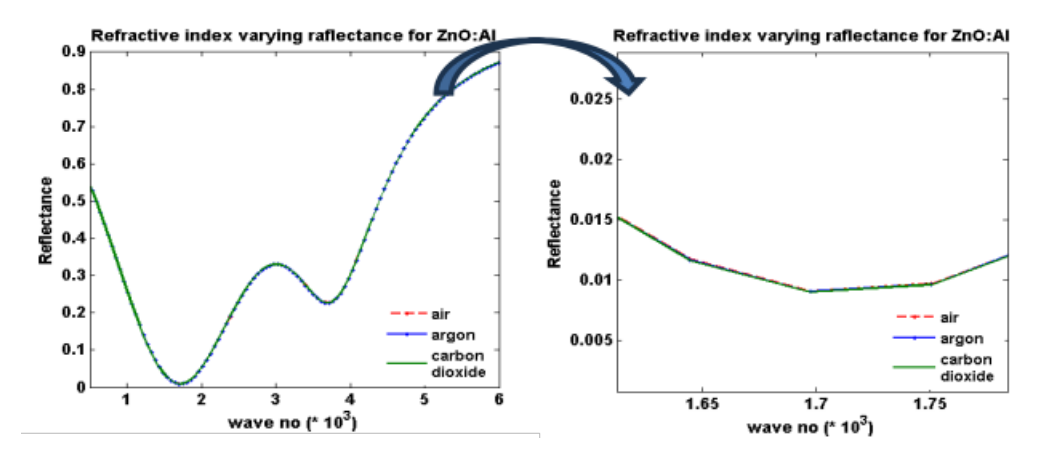


Figure 7: Variation of Reflectance with the wave number for 50 nm AZO taking the ambient material of Kretschmann configuration as air, argon, and CO2.

If the ambient material in the Kretschmann Configuration is varied from air to any gaseous medium like argon and carbon di oxide then there is a small variation in the resonance position which is described in Figure 6. The variation of the Reflectance at resonance is shown in the zoomed portion. When the refractive index of the ambient material is varied that means if the ambient material is taken as aqueous material like water and ethanol then the resonance of the collective oscillations with the incident light will happen for the incident angle above 400 if the film thickness taken is taken as 50 nm. The variation of the response of SPR with the different ambient material is described in the Figure. 6 and 7. When the ambient material is water, then the resonance occurs at $3926 \ cm - 1$. At this energy the reflectance at the receiving end is 6.4%. There is another case investigated, when the surrounding material is ethanol, then the resonance occurs at $1698 \ cm - 1$ with the reflectance 1.06%.

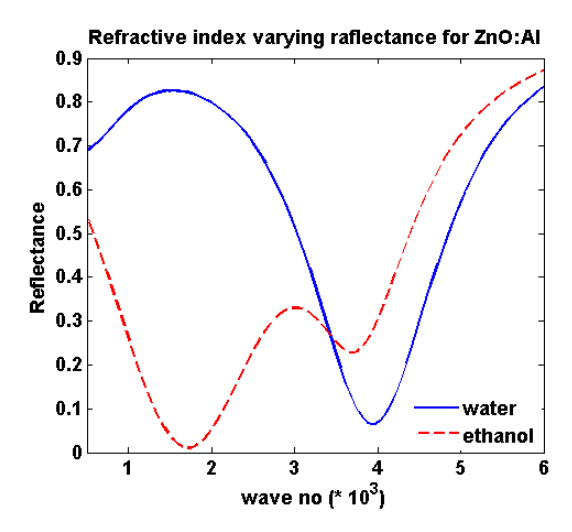


Figure 8: Variation of Reflectance with the wave number for 50 nm AZO taking the ambient material of Kretschmann configuration as water and ethanol

III.d Surface Plasmon Reflectance Profile for GZO:

The coupling of incident optical radiation with the oscillations of conduction electrons i.e. Surface Plasmons is demonstrated in Figure 8 for ZnO:Ga film in Kretschmann configuration for different thickness of the film. The increment of the thickness of the ZnO:Ga film effects the reflectance of the light detected from the Kretschmann configuration as can be visualized from Figure 8.

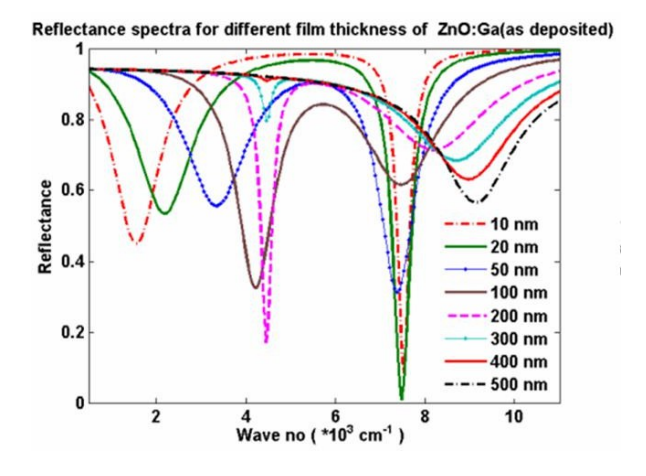


Figure 9: Reflectance as a function of wave number with the variation of thickness of ZnO:Ga layer

The excitation probability of electrons in Ga-doped ZnO (GZO) thin films exhibits a strong thickness dependence when irradiated at 45° incidence, with films below 50 nm demonstrating significantly enhanced interaction with the incident beam compared to thicker counterparts. Surface plasmon resonance (SPR) characterization reveals that films up to 200 nm thickness support coherent charge density oscillations, as evidenced by characteristic reflectance minima in spectroscopic measurements.

A 20 nm as-deposited GZO film (2 at% Ga) displays a pronounced SPR dip at $7480\,\mathrm{cm^{-1}}$ (plasmon frequency) with 0.73% reflectance minimum under 45° excitation, while angular variation studies show this resonance shifts to $7427\,\mathrm{cm^{-1}}$ with approximately 77% transmission through $50\,\mathrm{nm}$ films. Thicker

films exhibit modified plasmonic behavior, with 100 nm GZO showing resonance at $690 \,\mathrm{cm}^{-1}$ (2.77% reflectance) and 150 nm films demonstrating angular-dependent resonance shifting from $4403 \,\mathrm{cm}^{-1}$ (2.3% reflectance) at 45° to $6419 \,\mathrm{cm}^{-1}$ (0.233% reflectance) at 69° incidence.

The observation of dual-peak resonance at 45° incidence for films $\leq 150\,\mathrm{nm}$ contrasts with single resonance peaks in thicker films, suggesting thickness-dependent mode coupling. Notably, the complete disappearance of SPR features beyond 200 nm film thickness indicates a critical threshold where the film dimension exceeds the effective surface plasmon propagation length, consistent with theoretical predictions of plasmon damping in optically thick media. These findings demonstrate the tunability of plasmonic response in GZO thin films through precise thickness control and excitation geometry optimization.

III.e Sensor performance of GZO and related sensitivity issues:

The sensing application of ZnO:Ga for different samples of various refractive indices in the proposed structure is studied in the Figure 9 and 10. The dip shift on the reflection spectrum is used to detect the sample in terms of refractive index.

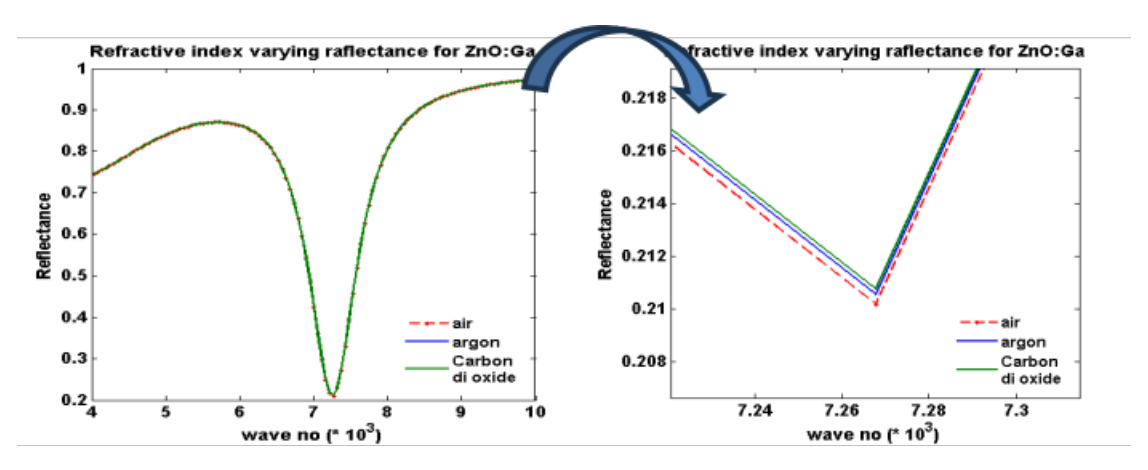


Figure 10: Variation of Reflectance with the wave number for 50 nm GZO taking the ambient material of Kretschmann configuration as air, argon, and CO₂.

When the refractive index of the ambient material is varied that means if the ambient material is taken as aqueous material like water and ethanol then the resonance of the collective oscillations with the incident light will happen for the incident angle above 500 if the film thickness taken is taken as 50 nm. The variation of the response of SPR with the different ambient material is described in the Figure 6. When the ambient material is water, then the resonance occurs at 7586 cm-1. At this energy the reflectance at the receiving end is 48.7%. There is another case investigated, when the surrounding material is ethanol, then the resonance occurs at 7321 cm-1 with the reflectance 40.02%.

The sensitivity of the measurement system can be quantified by observing the shift in resonance wavenumber corresponding to changes in the sample's refractive index. Figure 11 presents reflectance spectra for various samples with different refractive indices as indicated in the legend. While the resonance shifts are not immediately apparent in the full-scale spectra, closer examination of the magnified resonance dips reveals a clear trend - the resonant wavenumber systematically increases with higher sample refractive indices. This behavior demonstrates the expected positive correlation between refractive index and plasmon resonance position, where modifications to the dielectric environment surrounding the plasmonic material induce measurable changes in the surface plasmon dispersion characteristics. The magnitude of these wavenumber shifts, though subtle in the overall spectra, becomes distinctly measurable when analyzing the zoomed resonance features, confirming the fundamental

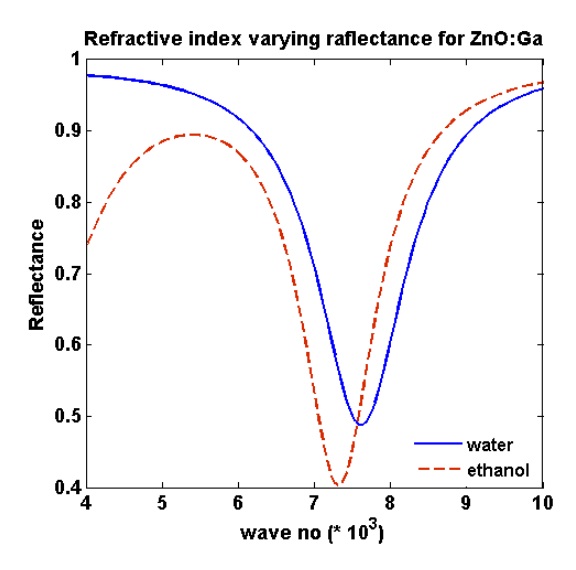


Figure 11: Variation of Reflectance with the wave number for 50 nm GZO taking the ambient material of Kretschmann configuration as water and ethanol.

sensitivity of the plasmonic system to refractive index variations. This observation aligns with established principles of surface plasmon resonance sensing, where the resonant condition depends critically on the dielectric properties of the adjacent medium.

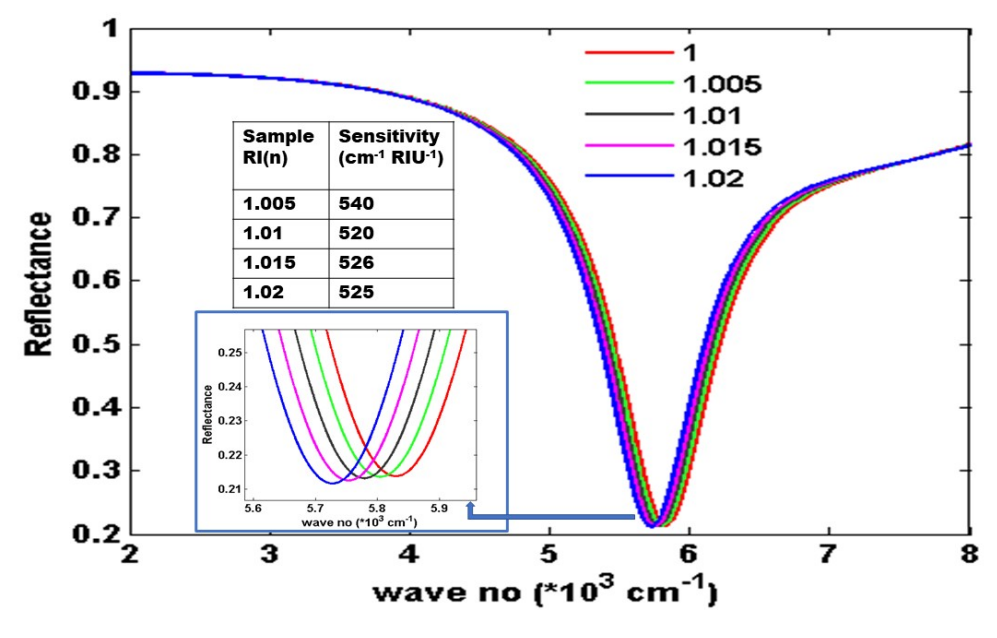


Figure 12: Sensing of gaseous samples using as-deposited ZnO:Ga films of thickness 150nm. The inset in fig is magnified view of the dip of resonances in reflection. Refractive index sensitivities obtained by considering air as reference.

If the sensitivity application is studied for 150nm Ga dopped ZnO when the electromagnetic radiation

is incident on the Kretschmann configuration, using different gaseous samples, then also it can be noticed that Sensitivity of the as deposited state is higher than that of annealed state for a particular sample as tabulated in Figure 11. This implies again that measurements with as deposited layer of 150nm GZO is sensitive to the different ambient materials of having different refractive indices and can be used as plasmonic material in Sensors.

IV Conclusions

The optical properties of Al-doped and Ga-doped zinc oxide (ZnO:Al and ZnO:Ga) thin films exhibit distinct surface plasmon resonance (SPR) characteristics when excited under specific conditions of incident angle and film thickness. Both materials demonstrate a transition between opaque and transparent states depending on these parameters, with particular combinations yielding dual-peak resonance behavior upon interaction with external light.

This study examines the relationship between incident radiation wavenumber and reflectance for various thicknesses of these metal oxide layers. The analysis reveals that the resonant reflectivity minimum, corresponding to SPR excitation, shows significant dependence on two key factors: the angle of incident radiation and the physical thickness of the metal oxide film. Notably, the SPR response shifts systematically with variations in either parameter.

The experimental results demonstrate that both ZnO:Al and as-deposited Ga-doped ZnO (GZO) layers exhibit measurable sensitivity to changes in surrounding dielectric environments characterized by different refractive indices. This responsive behavior to ambient conditions suggests these materials have potential applications as active components in plasmonic sensing devices. The tunable nature of their SPR characteristics, particularly the angular and thickness-dependent responses, provides a versatile platform for optical sensing applications where detection of refractive index changes is required. The observed dual-peak resonance phenomenon in specific configurations further enhances their utility for multi-parameter sensing applications.

References

- [1] B. Rech and H. Wagner. Potential of amorphous silicon for solar cells. *Appl. Phys. A. Mater. Sci. Process*, 69(2):155, 1999.
- [2] M. Zeman, R. A. C. M. M. van Swaaij, J. W. Metselaar, and R. E. I. Schropp. Optical modeling of a-si:h solar cells with rough interfaces: Effect of back contact and interface roughness. *Journal* of Applied Physics, 88(11):6436, 2000.
- [3] S. Ferlauto, G. M. Ferreira, J. M. Pearce, C. R. Wronski, R. W. Collins, X. Deng, and G. Ganguly. Analytical model for the optical functions of amorphous semiconductors from the near-infrared to ultraviolet: Applications in thin film photovoltaics. *Journal of Applied Physics*, 92(5):2424, 2002.
- [4] S. Franzen, C. Rhodes, M. Cerruti, R. W. Gerber, M. Losego, J. P. Maria, and D. E. Aspenes. Plasmonic phenomena in indium tin oxide and ito-au hybrid films. *Opt. Lett.*, 34(18):2867, 2009.
- [5] S. Franzen. Surface plasmon polaritons and screened plasma absorption in indium:tin oxide compared to silver and gold. J. Phys. Chem. C, 112(15):6027, 2008.
- [6] S. H. Brewer and S. Franzen. Optical properties of indium tin oxide and fluorine-doped tin oxide surfaces: correlation of reflectivity, skin depth, and plasmon frequency with conductivity. J. Alloys Compd., 338:73, 2002.
- [7] M. D. Losego, A. Y. Efremenko, C. L. Rhodes, M. G. Cerruti, S. Franzen, and J. P. Maria. Conductive oxide thin films: Model systems for understanding and controlling surface plasmon resonance. J. Appl. Phys., 106(2):024903, 2009.

- [8] C. Rhodes, S. Franzen, J. P. Maria, M. Losego, D. N. Leonard, B. Laughlin, G. Duscher, and S. Weibel. Surface plasmon resonance in conducting metal oxides. *J. Appl. Phys.*, 100:054905, 2006.
- [9] C. Rhodes, M. Cerruti, A. Efremenko, M. Losego, D. E. Aspnes, J. P. Maria, and S. Franzen. Dependence of plasmon polaritons on the thickness of indium tin oxide thin films. *J. Appl. Phys.*, 103(9):0931081, 2008.
- [10] U. Chowdhury, P. Mandi, R. Mukherjee, S. Chandra, S. Sutradhar, S. Kumar, and P. S. Maji. Dual self-referenced refractive index sensor utilizing tamm plasmons in photonic quasicrystal for multistage malaria parasite detection. *Plasmonics*, pages 10–1007, 2024.
- [11] K. H. Kim, K. C. Park, and D. Y. Ma. Structural, electrical and optical properties of aluminum doped zinc oxide films prepared by radio frequency magnetron sputtering. J. Appl. Phys., 81:7764, 1997.
- [12] I. Hamberg and C. G. Granqvist. Evaporated sn-doped in 203 films: Basic optical properties and applications to energy-efficient windows. J. Appl. Phys., 60:123, 1986.
- [13] A. J. Hoffman, L. Alekseyev, S. S. Howard, K. J. Franz, D. Wasserman, V. A. Podolskiy, E. E. Narimanov, D. L. Sivco, and C. Gmachl. Negative refraction in semiconductor metamaterials. *Nat. Mater.*, 6:946, 2007.
- [14] J. A. Schuller, R. Zia, T. Taubner, and M. L. Brongersma. Dielectric metamaterials based on electric and magnetic resonances of silicon carbide particles. *Phys. Rev. Lett.*, 99:107401, 2007.
- [15] S. Chatterjee, R. Mukherjee, S. Chandra, A. R. Maity, S. Kumar, and P. S. Maji. Harnessing tamm-plasmon polaritons in cantor sequence photonic quasicrystals for enhanced cancer cell detection. *Plasmonics*, pages 10–1007, 2024.
- [16] W. N. Hansen. Electric fields produced by the propagation of plane coherent electromagnetic radiation in a stratified medium. J. Opt. Soc. Am., 58(3):380, 1968.
- [17] J. P. Marton and B. D. Jordan. Optical properties of aggregated metal systems: interband transitions. *Phys. Rev. B*, 15:1719, 1977.